

CHAPTER 4

ADAPTIVE COMPUTATION OF GAIN MATRICES

In the last chapter we showed a method to design a modal filter that separated the vibration signal of a structure into its modal coordinates. Figure 2.7 shows the configuration of the sensor. In particular, it shows that the outputs of the sensor segments are multiplied by a gain matrix to produce the modal coordinates in real time. Equation (2.40) shows that the gain matrix is the inverse of the segment output matrix, which in turn is calculated from the mode shapes of the structure.

The analytical methods we have presented so far for computing segment weights for modal sensors rely on precise knowledge of the mode shapes of the structures. The dependence of precise knowledge of mode shapes has some drawbacks. First, if the actual mode shapes of the structure are not exactly the same as the mode shapes used in the calculation of the gain matrix, the modal filters will fail to ‘cleanly filter out’ the modes that they should filter out. Second, it is impossible to build a modal sensor without doing a thorough testing and analysis of the modal properties of the structures. Mode shapes of real structures are usually obtained after much computation, e.g., finite element methods or modal analysis. Calculation of gain matrices of the modal sensors must be done after the calculation of the mode shapes.

Sometimes the following situations preclude the use of currently available techniques to design modal sensors:

1. The modal properties (natural frequencies, modal damping ratios, and modal residues) are not known precisely.
2. The global modal properties (natural frequencies, modal damping ratios) are known, but local properties (modal participation factors) are not known. This means that we do not know the mode shapes of the structures. As mentioned above, mode shapes are necessary in the computation of the gain matrix for the modal filters.
3. Very limited modal information of the structure is available. For example, we only know the number of modes in the frequency range of interest, but we don’t know the natural frequencies, modal damping ratios, and mode shapes of the structure.

In this chapter we shall discuss

1. How the design of modal filters is affected by incompleteness of knowledge of the modal properties.
2. Techniques to compensate for the inaccuracies of the modal sensors
3. Methods to extract modal properties from the structure using the segmented sensor

4.1 Effects of Inaccurate Mode Shapes

In this section we shall use only a mode-3 sensor as an example. This sensor is designed to be sensitive only to the 3rd vibration mode, and filter out signals from all other modes.

We showed in the previous chapter that the output of the mode-3 sensor consists only of the third modal coordinate of the structural vibration. When the structure parameters change from their original ‘design’ values, the FRF from force to the output of the segmented sensor fails to exhibit a Single-Degree-of-Freedom (SDOF) response as the sensor is designed to perform. In this section we discuss how deviations from the design modal properties affect the performance of the modal sensors.

Consider the response of a segmented sensor designed to sense the third modal coordinate of the simply supported beam with torsion spring. Figure 4.1 shows the magnitudes of the FRF’s from force to sensor output. The sensor is designed for a the beam in Section 3.1 with torsion spring stiffness $T^* = 1$. However, if the structure’s actual torsion spring stiffness is $T^* = 10$, the sensor response deviates from the ideal SDOF response. Specifically, the differences between the two responses are:

1. The resonance frequency of the $T^* = 10$ structure is higher than that of the $T^* = 1$ structure.
2. Resonance peaks appear in the $T^* = 10$ response at the resonance frequencies of the modes other than mode 3. These modes should be filtered out by the mode-3 sensor.

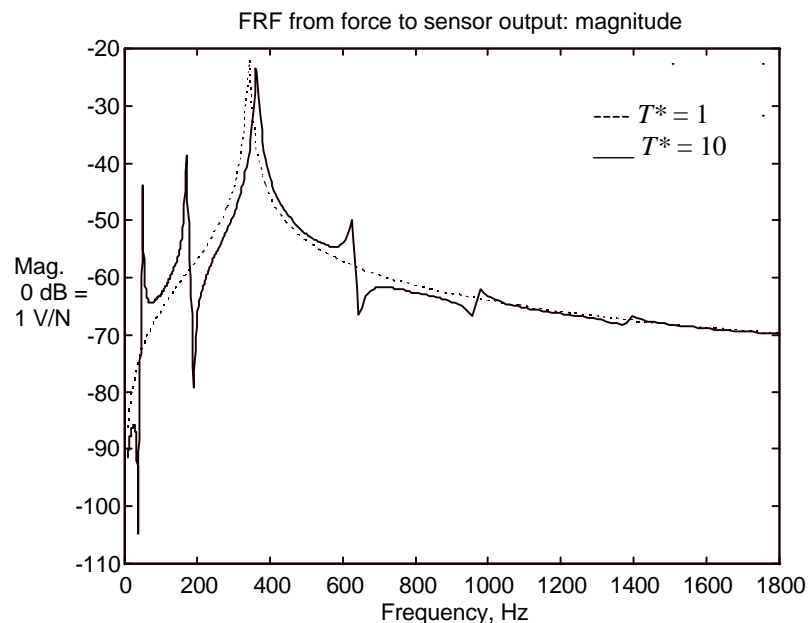


Figure 4.1 Magnitudes of the responses of the sensor on the $T^*= 1$ structure and on the $T^*=10$ structure

Figure 4.2 shows the phases of the FRF's. The $T^* = 1$ response phase rolls off from 90^0 to -90^0 in the region around the third resonance frequency. At frequencies below this resonance frequency region, the phase is 90^0 ; and at frequencies higher than the resonance frequency region the phase is -90^0 . The phase of the $T^* = 10$ response rolls off at a higher frequency than the third resonance frequency of the $T^* = 1$ structure. At the resonance frequencies of other modes, the phase is neither 90^0 nor -90^0 .

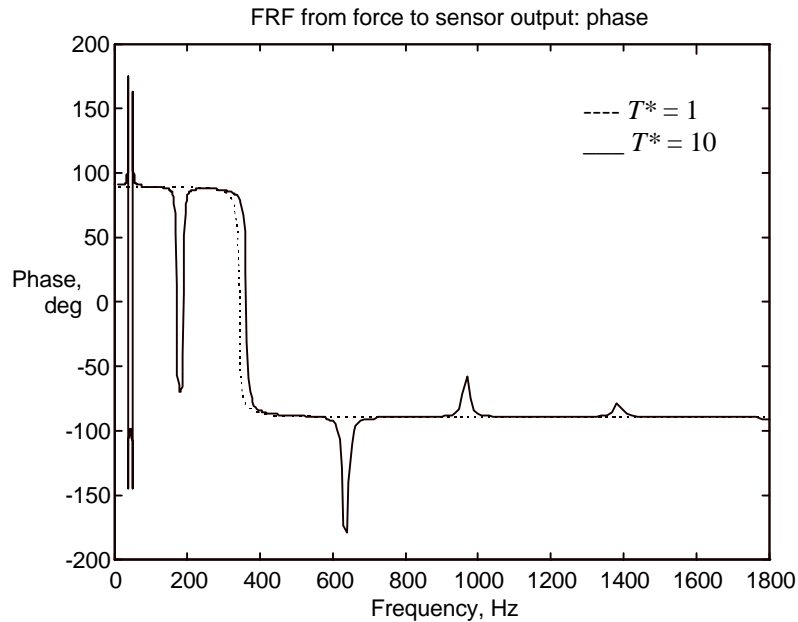


Figure 4.2 Phases of the responses of the sensor on the $T^* = 1$ structure and on the $T^* = 10$ structure

Figure 4.3 shows the real part of the FRF's. The real part of the $T^* = 1$ FRF has a peak in the region around the third resonance frequency. At frequencies below and above this resonance frequency region, the real part is zero. The real part of the $T^* = 10$ response, on the other hand, fails to stay at zero outside the resonance frequency region.

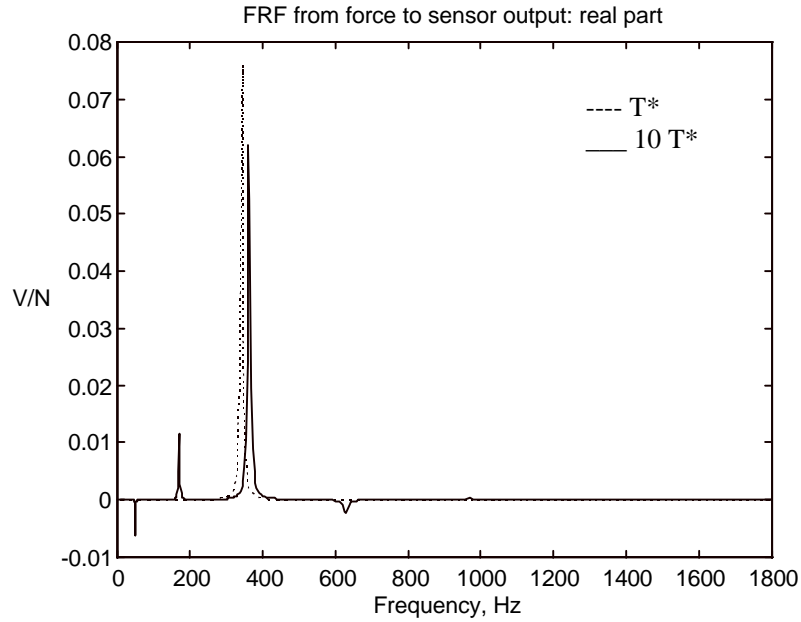


Figure 4.3 Real parts of the responses of the sensor on the $T^* = 1$ structure and on the $T^* = 10$ structure.

4.2 Adaptive Design of Modal Sensors

The main thrust of this research is the development of a method to design a modal sensor for a continuous structure without much prior knowledge of the modal properties of the structure. Designing a modal sensor for a continuous structure means calculating the sensor gain matrix \mathbf{W} . In this section, we shall develop a such a method using adaptive signal processing techniques.

4.2.1 Correlation Between Modal Coordinates

The method we will develop is based on the correlations between modal coordinates. The first step in developing the design method is to investigate these correlations. Figure 4.4 shows two second order filters with different natural frequencies. A random input is common to both filters. We shall investigate the correlations between the two outputs.

Let us call the outputs of the modal filters $\dot{h}_i(k)$ and $\dot{h}_j(k)$, and assume that these are modal coordinates. Let us define the *cross correlation function* between the two modal coordinates at *zero lag* as

$$\mathbf{R}_{ij} = E[\dot{h}_i(k)\dot{h}_j(k)], \quad (4.1)$$

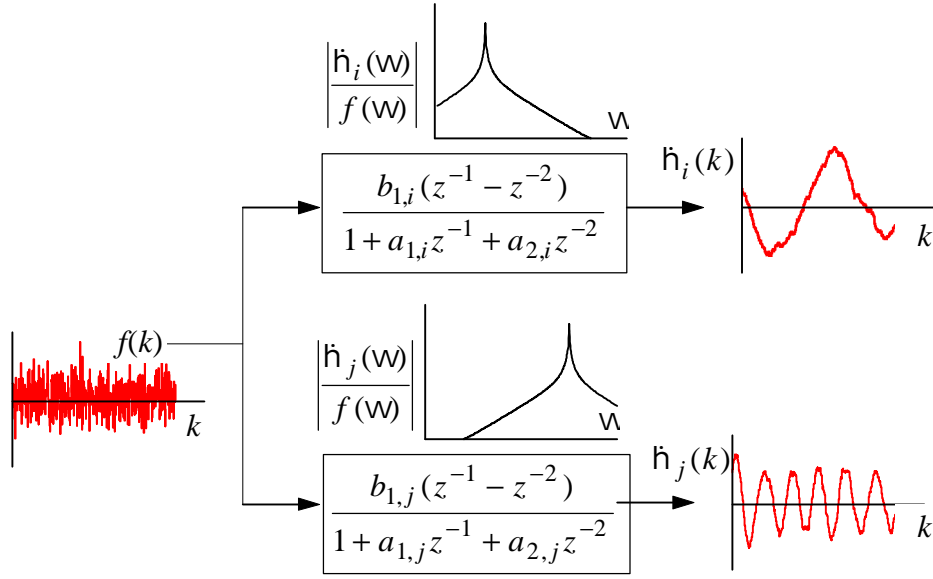


Figure 4.4 Modal responses to random excitation.

where $E[\cdot]$ denotes expectation. Strictly speaking, the expectation should be obtained by ensemble averaging. However, we assume that the modal coordinates are stationary and ergodic. Therefore, we can replace the ensemble averaging with time averaging, and we can rewrite the last equation as

$$\mathbf{R}_{ij} = \frac{1}{k} \lim_{k \rightarrow \infty} \sum_{h=1}^k \dot{h}_i(h) \dot{h}_j(h). \quad (4.2)$$

In the implementation, we can only approximate the expected value by choosing a large but finite number for k and possibly checking for convergence. To avoid storage of all past records, we use a recursive formula for the above approximation as

$$\mathbf{R}_{ij}(k) = \frac{1}{k} \left\{ (k-1)\mathbf{R}_{ij}(k-1) + \dot{h}_i(k)\dot{h}_j(k) \right\}, \quad (4.3)$$

where the index k denotes the time step in which \mathbf{R}_{ij} is computed. This index notation is different from the usual notation for correlation functions, where the index k would normally show the delay between $\dot{h}_i(k)$ and $\dot{h}_j(k)$.

If $\dot{h}_i(k)$ and $\dot{h}_j(k)$ are modal coordinates, then they must be orthogonal to each other, therefore, uncorrelated. Thus, the correlation between the two modal coordinates must be zero.

$$\lim_{k \rightarrow \infty} \mathbf{R}_{ij}(k) = 0; \quad i \neq j. \quad (4.4)$$

This principle will be used to develop a method to separate the structural response into its modal coordinates.

Simulation of the filters in Fig. 4.4 with a Gaussian zero-mean random input results in signals in Fig. 4.5 for modes 1 and 3. The product of the two outputs $\dot{h}_1(k)$ and $\dot{h}_3(k)$ is averaged over time to estimate the zero-lag cross correlation function, $\mathbf{R}_{13}(k)$. As expected, the computed zero-lag cross correlation between the two modal coordinates approaches zero as more and more samples are included in the computation.

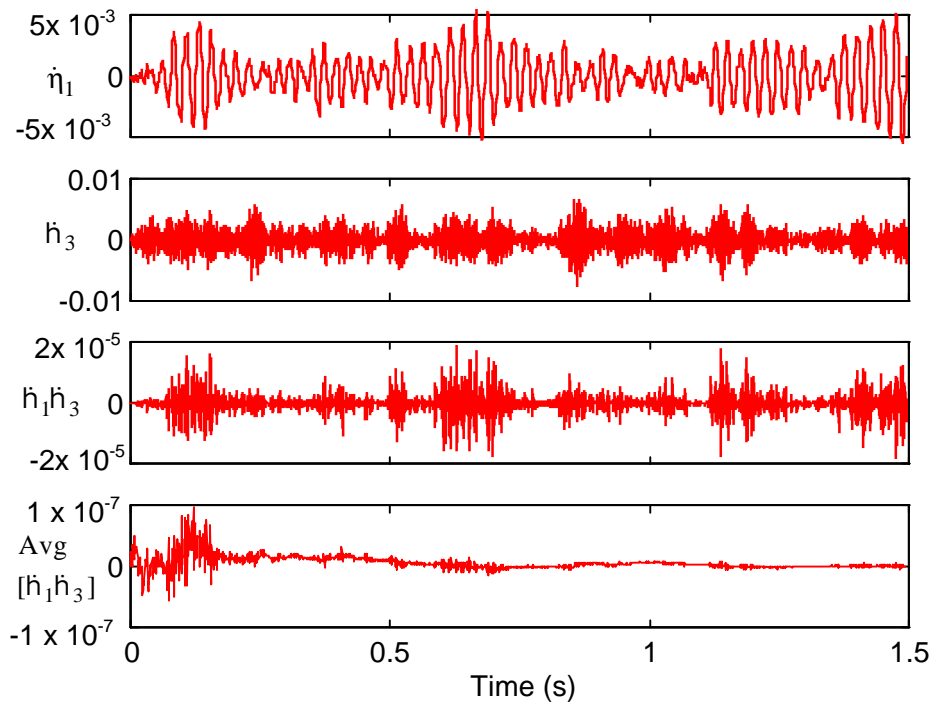


Figure 4.5 Mode-1 coordinate, mode-3 coordinate, product of mode-1 and mode-3 coordinates, average of product of mode-1 and mode-3 coordinates.

4.2.2 Adaptive Computation of Sensor Gain Matrix

We can compute the zero-lag correlations between all modes of a structure, and define a matrix of correlations among sensor outputs at zero lag as

$$\mathbf{R} = \begin{bmatrix} \mathbf{R}_{11} & \mathbf{R}_{12} & \cdots & \mathbf{R}_{1M} \\ \mathbf{R}_{12} & & & \vdots \\ \vdots & & & \\ \mathbf{R}_{M1} & \cdots & & \mathbf{R}_{MM} \end{bmatrix}, \quad (4.5)$$

where the components \mathbf{R}_{ij} , $i = 1, \dots, M$, $j = 1, \dots, M$, are defined as in Eq. (4.2), and computed as in Eq. (4.3). M is the number of modes included in calculations. Since the correlations between any different modes is zero, \mathbf{R} must be diagonal.

Now consider the system in Fig. 4.6. The correlations between the sensor outputs \hat{h}_m ($m = 1, \dots, M$) will form a diagonal matrix only if the sensor outputs are proportional to modal coordinates. This condition will be achieved only if the gain matrix \mathbf{W} has the correct components. If the gain matrix does not have the correct component, the correlations between the sensor outputs will not form a diagonal matrix. The foregoing notion can serve as a basis for developing algorithms to adjust the sensor gain matrix \mathbf{W} iteratively until the correlation matrix is diagonal. The development of such algorithms will be explained as follows.

Define the correlation between sensor outputs as

$$\mathbf{R} = \mathbf{E} \left[\begin{bmatrix} \hat{h}_1 \\ \vdots \\ \hat{h}_M \end{bmatrix} \begin{bmatrix} \hat{h}_1 & \cdots & \hat{h}_M \end{bmatrix} \right] \quad (4.6)$$

where M is the number of modes in the frequency range of interest. Substituting Eq. (2.32) into Eq. (4.6), we can express the correlation matrix as

$$\mathbf{R} = \mathbf{E}[\mathbf{W}\mathbf{V}\mathbf{V}^T\mathbf{W}^T]. \quad (4.7)$$

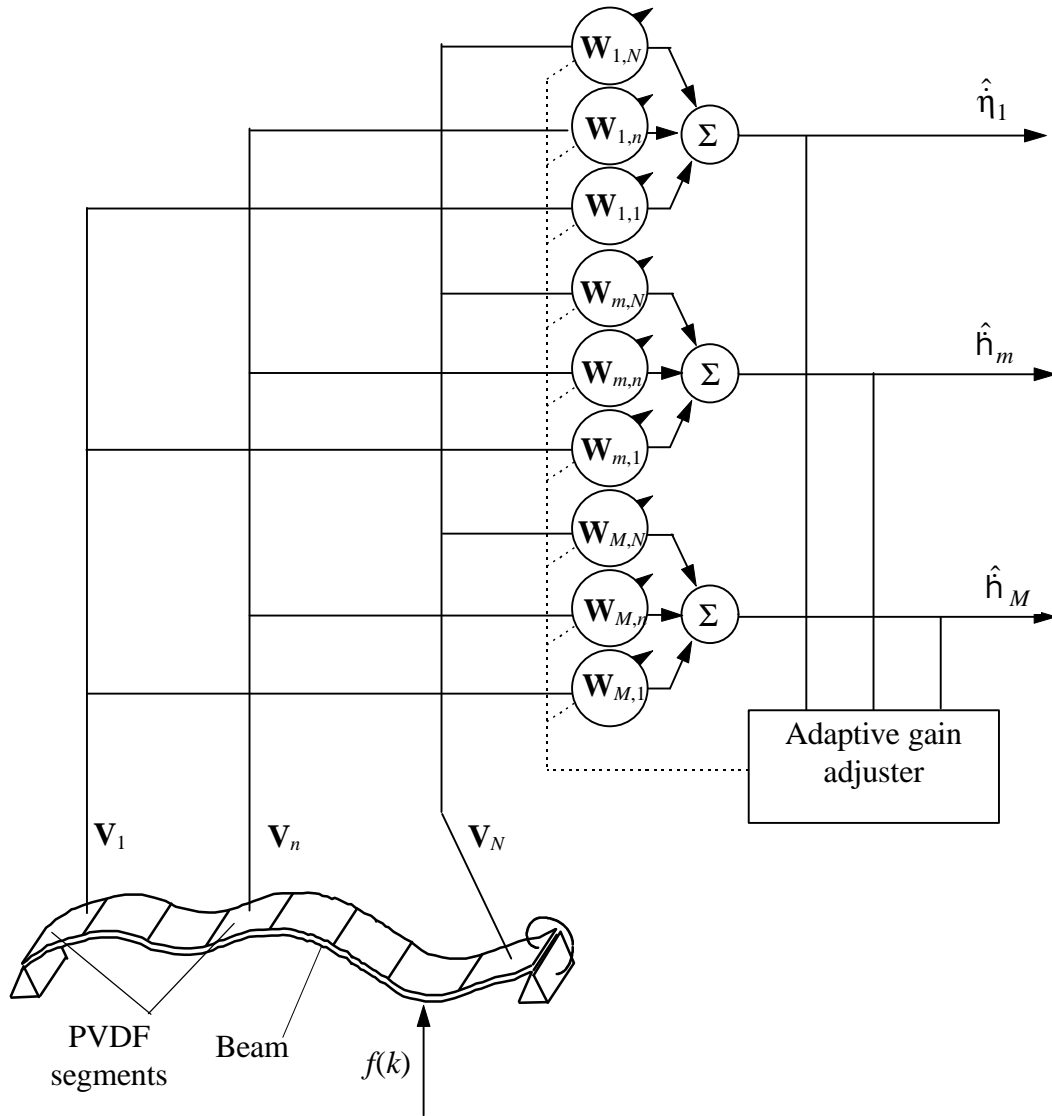


Figure 4.6 Adjusting sensor gain matrix to diagonalize correlation matrix.

In the adaptive system, the sensor gain matrix will be adjusted from time to time. However, the sensor gain matrix \mathbf{W} that transforms $E[\mathbf{V}\mathbf{V}^T]$ into modal coordinates is a constant matrix. Therefore, for the purpose of obtaining \mathbf{W} we can simplify Eq. (4.7) into

$$\mathbf{R} = \mathbf{W}E[\mathbf{V}\mathbf{V}^T]\mathbf{W}^T. \quad (4.8)$$

Next, we define the expected value term in the above equation as

$$\mathbf{S} = \mathbf{E}[\mathbf{V}\mathbf{V}^T]. \quad (4.9)$$

If \mathbf{S} is diagonalizable, with an eigenvector matrix

$$\mathbf{\Psi} = [y_1 \ \cdots \ y_M], \quad (4.10)$$

where y_m is the m^{th} eigenvector of \mathbf{S} , then the matrix $\mathbf{\Psi}^{-1}\mathbf{S}\mathbf{\Psi}$ is diagonal. Moreover, $\mathbf{\Psi}$ is an eigenvector matrix, so

$$\mathbf{\Psi}^{-1} = \mathbf{\Psi}^T. \quad (4.11)$$

Thus, to diagonalize the sensor output correlation matrix \mathbf{R} in Eq. (4.8) we can simply set the gain matrix to

$$\mathbf{W} = \mathbf{\Psi}^T. \quad (4.12)$$

4.3 Numerical Example

The above equation is a very important conclusion in this research. The equation states that: if we set the sensor gain matrix to the transpose of the eigenvector matrix of the expected values of the products between segment outputs, then the outputs of the sensor will be orthogonal to each other.

To verify the above theory, we simulate the system in Fig. 4.6 with a computation program shown in Fig. 4.7. The physical properties of the system are as in Subsection 3.1.1. The segment output correlation matrix \mathbf{S} in Eq. (4.9) is approximated with a recursive formula similar to Eq. (4.3). The sensor gain matrix \mathbf{W} is the transpose of the eigenvector matrix of \mathbf{S} . As the estimate for \mathbf{S} becomes closer to the true expected values of the correlation between the segment outputs, the sensor gain matrix \mathbf{W} in Eq. (4.12) becomes closer to a gain matrix that results in orthogonal sensor outputs. This means that the sensor output correlation matrix in Eq. (4.6) becomes closer to a diagonal matrix. The orthogonal sensor outputs will be proportional to the modal coordinates.

We run the above simulation with the beam example with a Gaussian random input force and obtain the following results. At the outset, $k = 16$, the sensor gain matrix \mathbf{W} (let us call this gain matrix $\mathbf{W}(16)$) is as shown in Fig. 4.8. Each plot shows the gains for one mode. This ‘early guess’

of sensor gain matrix \mathbf{W} does not really resemble the ideal sensor gain matrix in Fig. 4.9 (which is a rescaled version of Fig. 3.6.)

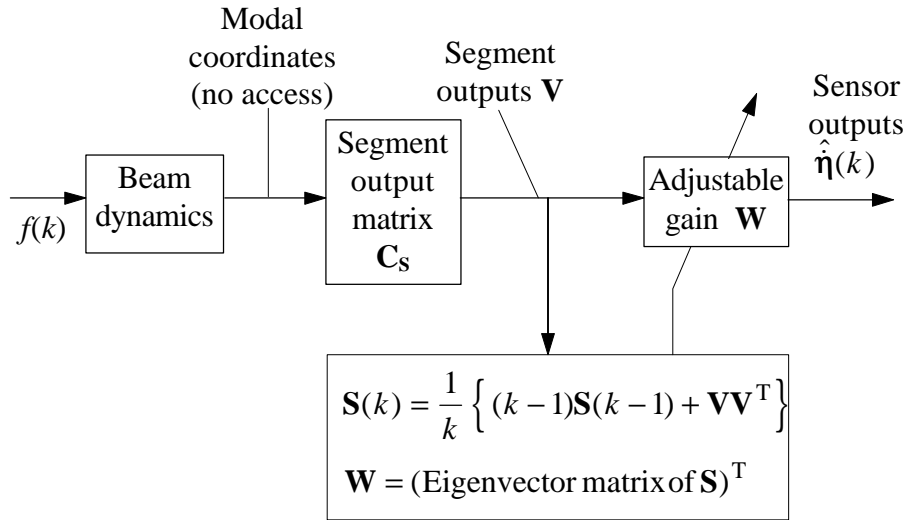


Figure 4.7 Sensor gain matrix adjustment using eigenvector matrix of segment output correlations.

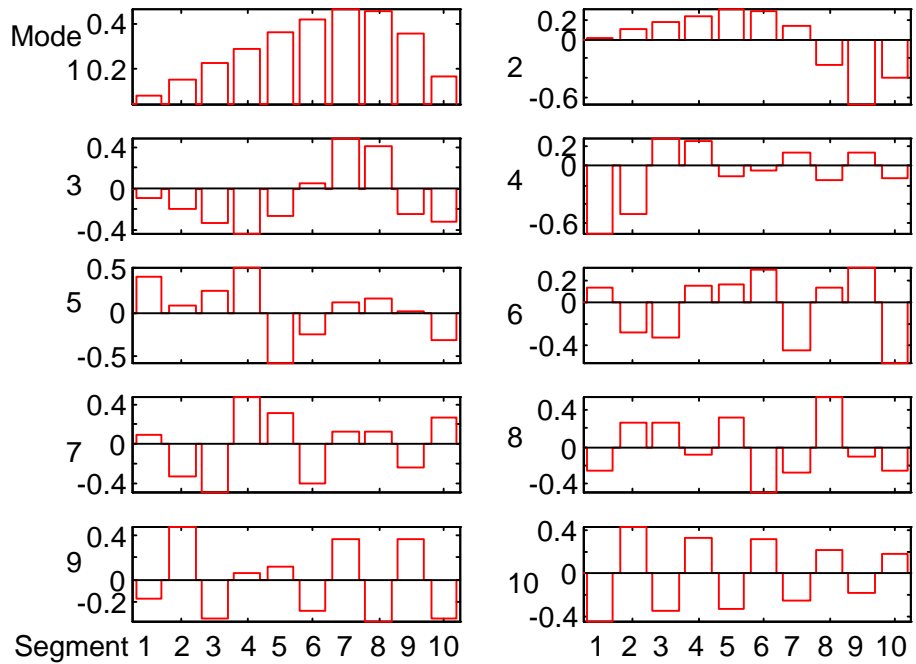


Figure 4.8 Sensor gain matrix computed with 16 sets of time data, $\mathbf{W}(16)$.

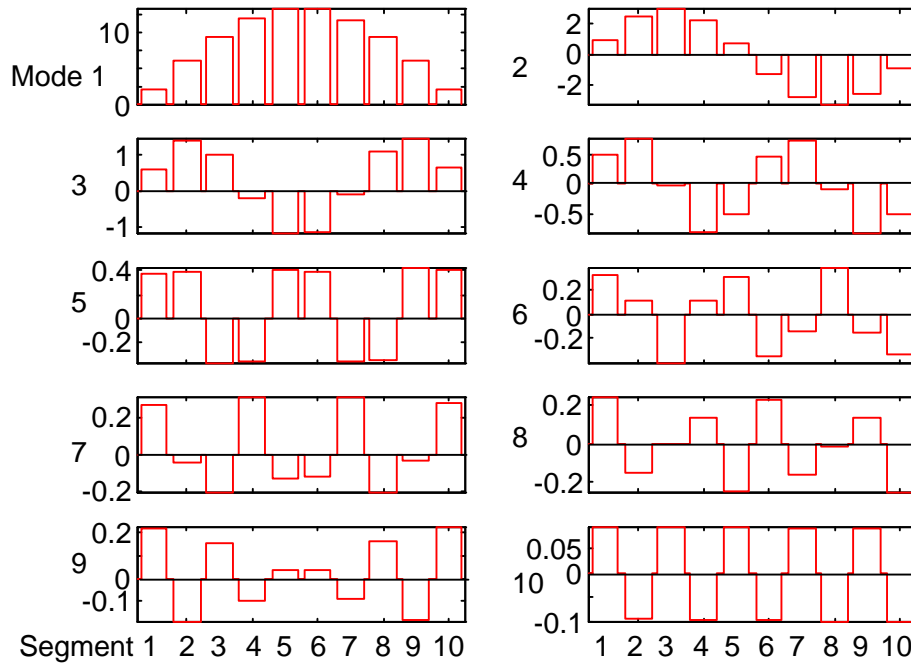


Figure 4.9 Ideal sensor gain matrix.

With a sensor gain matrix that is so different from the ideal, we cannot expect the sensor outputs to be uncorrelated. To verify this statement, we run another simulation with 8192 points using the gain matrix in Fig. 4.8. Then we compute the correlation matrix of the resulting sensor outputs. The correlation matrix is shown in Fig. 4.10.a. in a picture format suitable for showing symmetric matrices with large diagonal elements. The height of each bar in this figure shows the value of the corresponding component of the correlation matrix. Since the (10,10) component of the correlation matrix is much greater than the other components, the scaling of the heights obscure the depiction of the other components. Rescaling the picture as in Fig. 4.10.b gives a better idea of the relative values of the matrix components. Notice that the sensor output correlation matrix is far from being diagonal. This means that the sensor gain matrix results in sensor outputs that are not uncorrelated.

At time step $k = 256$, the sensor gain matrix is as shown in Fig. 4.11. It appears that the segment gains are starting to evolve towards the ideal gain matrix (Fig. 4.9). However, with this segment gain matrix, the output correlation matrix is still not diagonal (See Fig. 4.12.)

A question that naturally arises from the above examples is: How many time steps should be used to estimate the expected value of segment outputs (Eq. (4.9)) to obtain a sensor gain matrix (Eq. (4.12)) that will uncorrelate the sensor outputs? To answer this question, we need to go back to Eq. (4.1) and determine the number of time data points that will make Eq. (4.2) a reasonable

approximation to Eq. (4.1). To this end, we can check a few estimates for the correlation between different modal coordinates. We know that the correlation should be close to zero. If we examine Fig. 4.5 again, we can observe that the estimate for the correlation between $\hat{h}_1(k)$ and $\hat{h}_3(k)$ settles around zero after about 30 000 time data points. For $k > 30000$, this estimate is almost unaffected by large fluctuations in $\hat{h}_1(k)$ or $\hat{h}_3(k)$. We also know that $\hat{h}_1(k)$ is the most slowly varying modal coordinate of the system. Therefore, if the product of $\hat{h}_1(k)$ and another modal coordinate settles around zero, evidently other products of modal coordinates also settle around their expected values. Based on the above observation, we compute the sensor gain matrix \mathbf{W} using 32768 time-data points. The resulting sensor gain matrix is shown in Fig. 4.13. Notice that each row of this sensor gain matrix is very nearly proportional to the corresponding row in the ideal sensor gain matrix shown in Fig. 4.9. Figure 4.14 shows that correlation between the sensor outputs for this sensor gain matrix is almost diagonal.

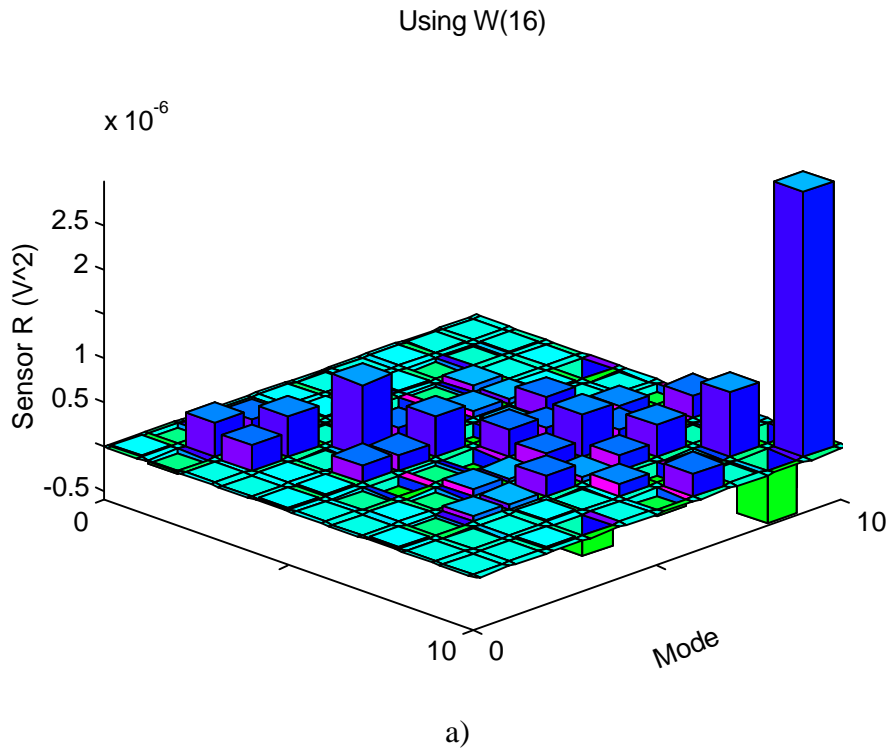


Figure 4.10.a Sensor output correlation matrix using $\mathbf{W}(16)$.
(Drawn to scale)

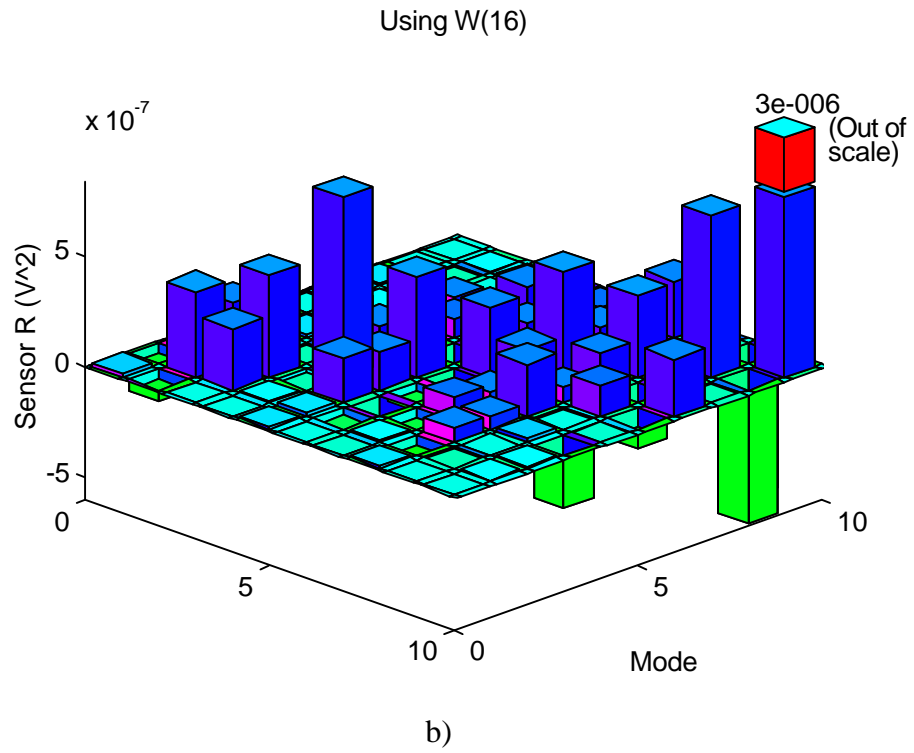


Figure 4.10.b Sensor output correlation matrix using $W(16)$.
(Not to scale)

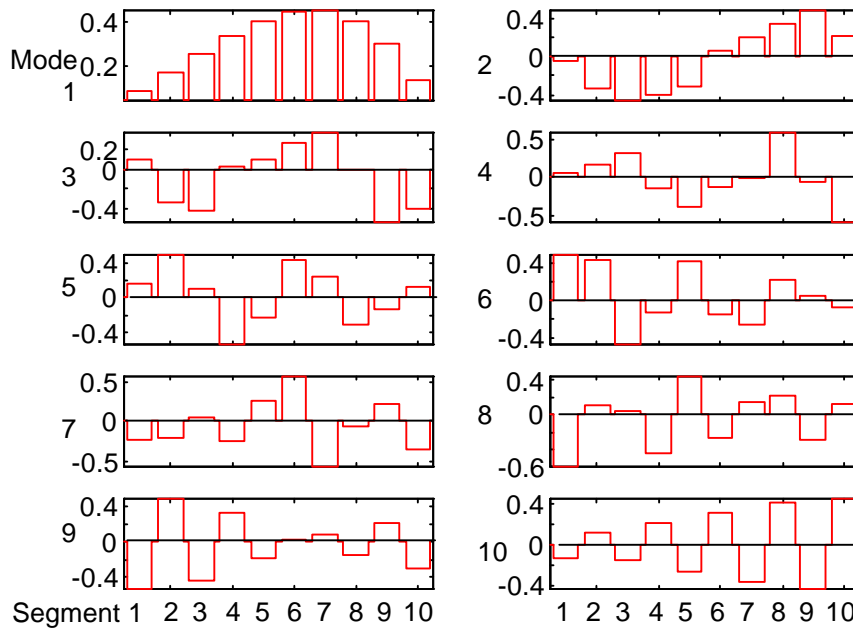


Figure 4.11 Sensor gain matrix $W(256)$.

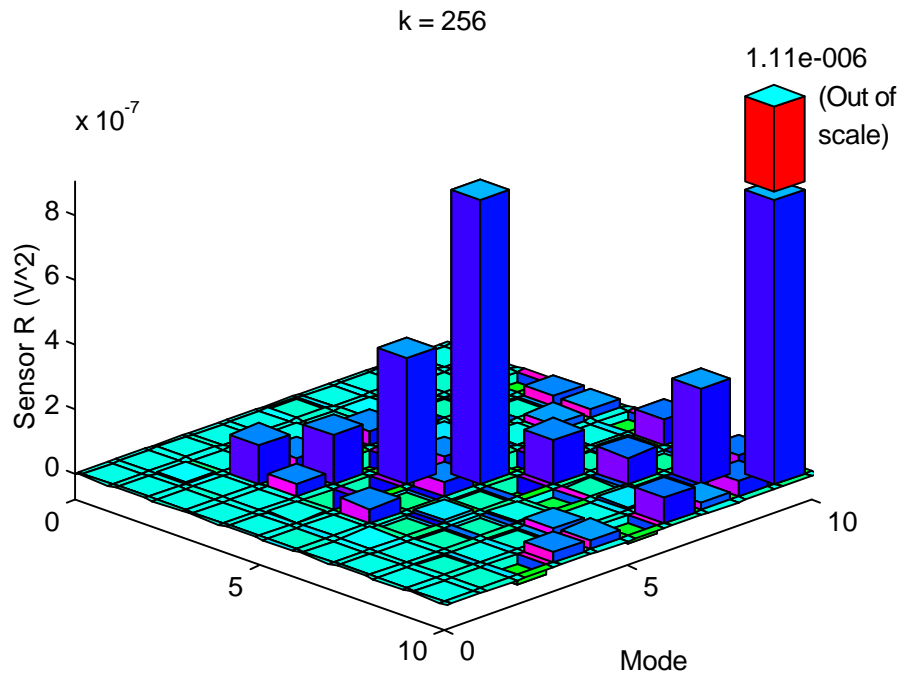


Figure 4.12 Sensor output correlation matrix resulting from $\mathbf{W}(256)$.

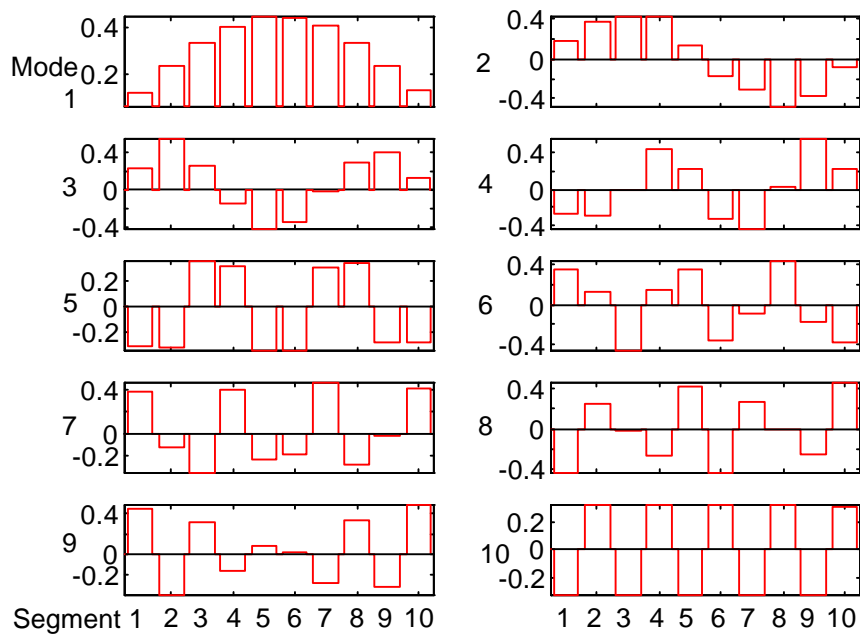


Figure 4.13 Sensor gain matrix calculated using 32768 time data points.

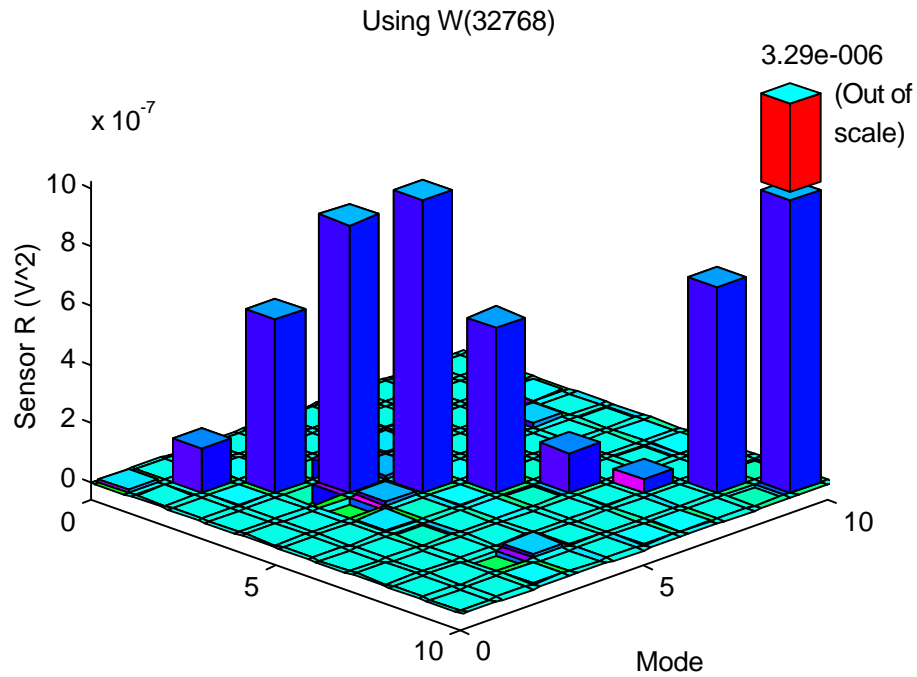


Figure 4.14 Sensor output correlation matrix resulting from $W(32768)$.

If we continue using more and more time points, we may obtain better estimate for the segment output correlation matrix and a better sensor gain matrix. However, the improvements may be marginal because the estimates for the correlations have settled around their theoretical values. For example, the sensor gain matrix obtained using 49152 time data points, shown in Fig. 4.15, is very close to the sensor gain matrix obtained using 32768 points, shown in Fig. 4.13. The sensor output correlation matrix obtained with 49152 time data points (Fig. 4.16) is also very similar to the corresponding matrix obtained with 32768 points (Fig. 4.14). Evidently, the correlations have settled around their theoretical values.

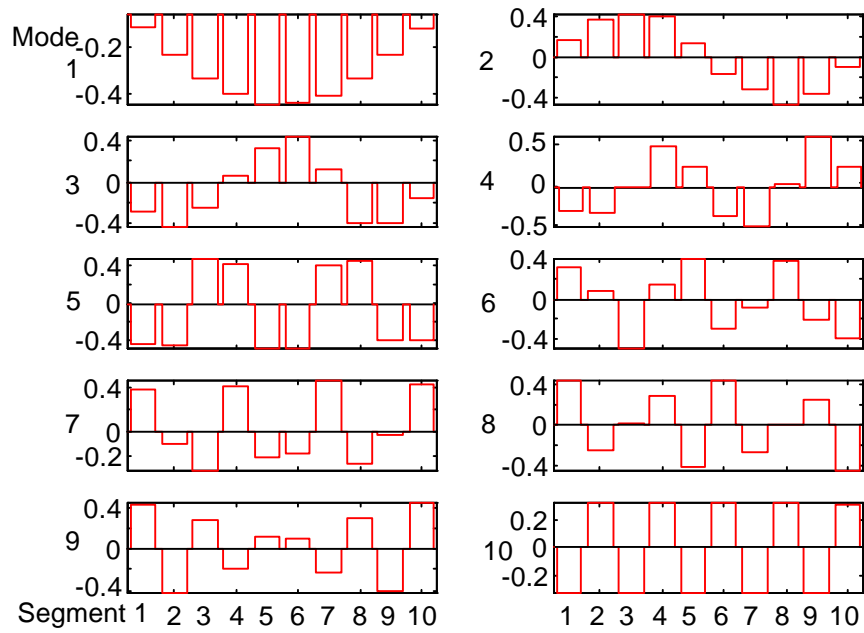


Figure 4.15 Sensor gain matrix calculated using 49152 time data points.

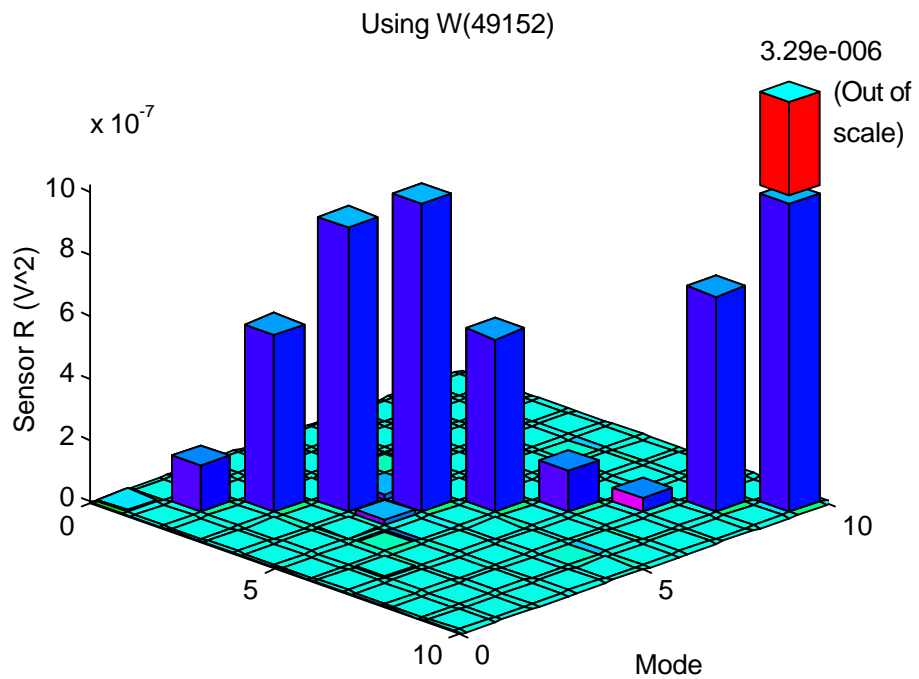


Figure 4.16 Sensor output correlation matrix resulting from $\mathbf{W}(49152)$.

Each row of the gain matrix represents a sensor that is supposed to sense only one particular modal coordinate and filter out other modal coordinates. The rows of the gain matrix obtained with the adaptive technique using 32768 time data points are not exactly proportional to the corresponding rows in the ideal gain matrix that we would obtain analytically if we knew the mode shapes of the structure. Therefore, the sensor outputs obtained with the adaptive sensor in Fig. 4.7 may not be exactly proportional to the ideal modal coordinates. To compare the sensor outputs to the ideal modal coordinates, we obtain the frequency response functions ($\hat{h}_m(\omega)/f(\omega)$, $m = 1, \dots, 10$) of the system in Fig. 4.7, and compare them with the frequency response functions ($\check{h}_m(\omega)/f(\omega)$, $m = 1, \dots, 10$) of the same system with the ideal gain matrix. The comparison is shown in Fig. 4.17.

Around the natural frequencies, the adaptive sensor outputs are nearly proportional to the modal coordinates. Away from the natural frequencies some of the adaptive sensor outputs are corrupted by signals from modes that the sensor should not be sensitive to. The imperfect filtering of other modes means that the sensor gain matrix still needs some refinement. A method to refine the sensor gain matrix will be presented in the next chapter. The important statement at this point is that the above numerical simulation and frequency-domain verification show that the sensor gain matrix computation scheme described in this chapter converges closely to the ideal sensor gain matrix. Thus, we have established the basis for a new method to compute the sensor gain matrix of a modal sensor without knowledge of the mode shapes of the structure.

Being in its conception, this method still needs much more development before it can be applied as a standard modal filtering technique. In the next chapter we will discuss the problems that must be solved to implement this method.

4.4 Chapter Summary

As mentioned in Chapter 1, most methods for designing modal sensors for structures rely on precise knowledge of the modal properties of the structures, especially the mode shapes. Modal sensors designed using inaccurate mode shape functions may not filter out undesired modes which the sensors are not supposed to sense. Some of the currently available methods may enable us to design a modal sensor without knowledge of the mode shapes. However, these methods require that we know the natural frequencies and modal damping of the structure. In this dissertation we attempt to develop another method to design a modal sensor without even knowing the above modal properties of the structure.

In this chapter we established the basis for such a method. This method is based on the fact that modal coordinates of a vibrating structure are uncorrelated to each other. In our case study, the sensor is composed of strain sensing segments. We produce the uncorrelated outputs by transforming the segment outputs with a correct sensor gain matrix. We obtain this gain matrix from the estimated expected values of the correlation between the segment outputs.

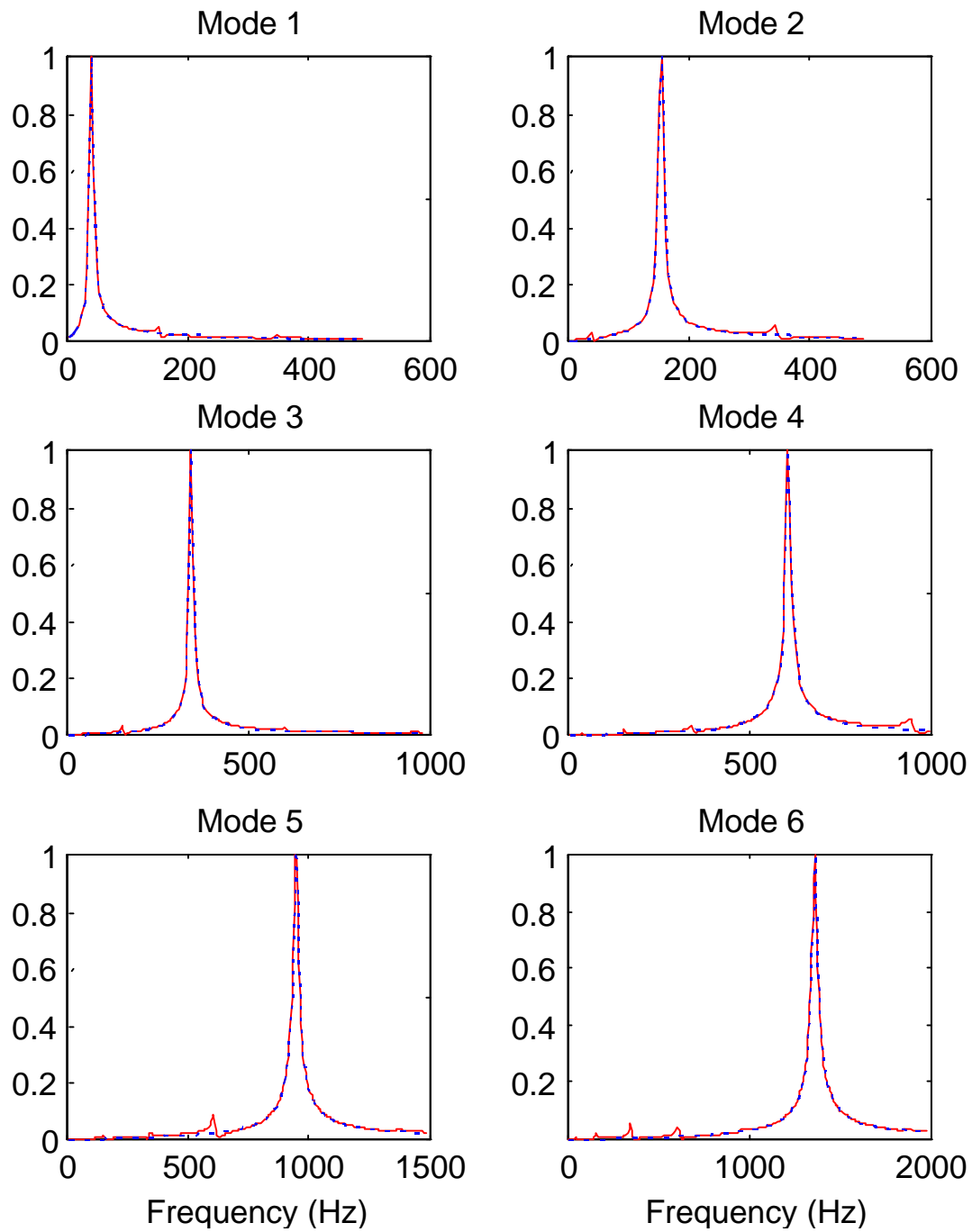


Figure 4.17 Magnitudes of adaptive sensor outputs (solid lines) and ideal modal coordinates (dotted lines).

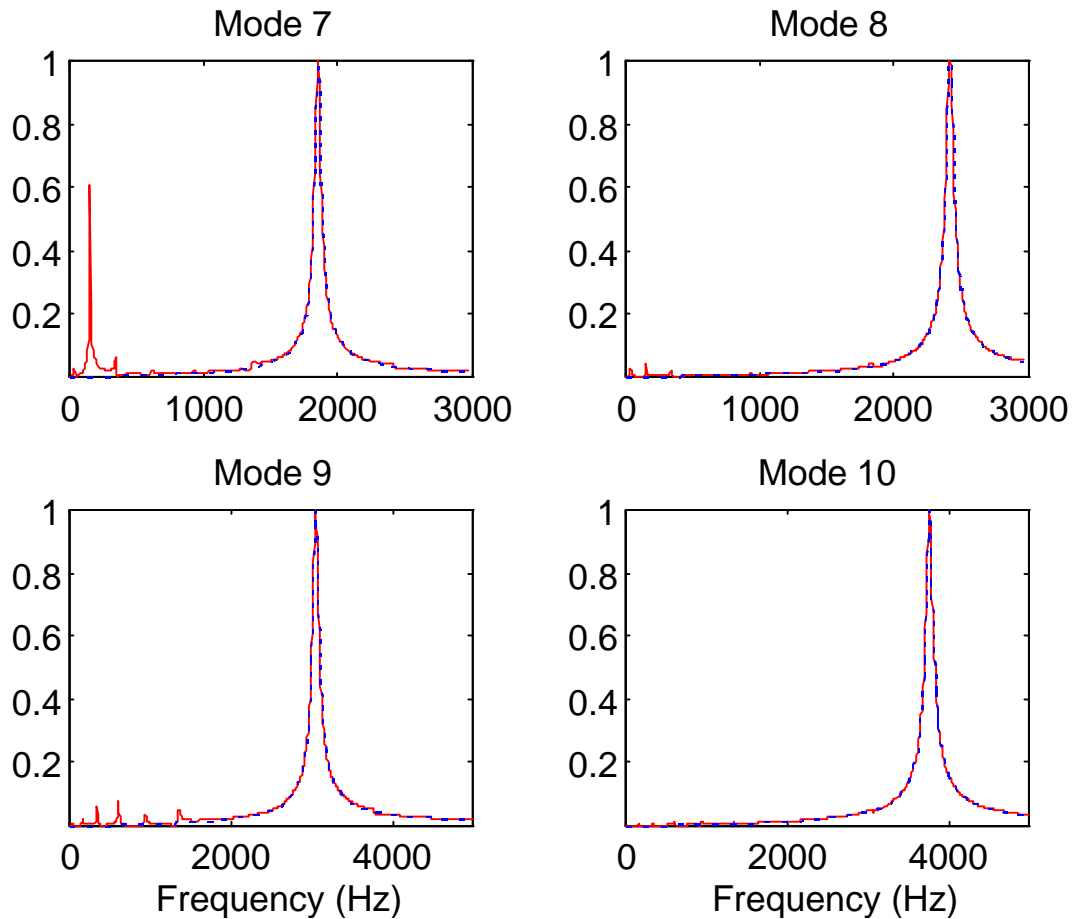


Figure 4.17 Magnitudes of adaptive sensor outputs (solid lines) and ideal modal coordinates (dotted lines).

We showed that the sensor outputs produced by the transformation with this sensor gain matrix are, indeed, uncorrelated to each other. We also showed that each row of the sensor gain matrix is proportional to the corresponding row in the ideal sensor gain matrix that would result from analytical calculation using known mode shape functions.

The sensor gain matrix that will produce modal coordinates can be shown to be equal to the eigenvector matrix of the segment output correlation matrix. The segment output correlation matrix is defined as a matrix that contains the correlations between the segment outputs at zero time lag. This segment output correlation matrix can be obtained on-line by processing the outputs of the sensor segments when the structure is excited with a persistent excitation such as Gaussian random force. These segment outputs are multiplied by each other. The products are averaged over time to estimate the expected values of the products. The estimation improves with

time as more data points are used to estimate the correlations. The resulting sensor gain matrix converges over time to the ideal sensor gain matrix.

The computation of the sensor gain matrix involves the computation of the eigenvector matrix of the segment output correlation matrix. In the application, the eigenvector computation must be done iteratively. However, the eigenvectors do not have to be updated frequently, since changes in the eigen-properties of the structure are generally very slow.

The FRF's from force to sensor outputs are generally proportional to the FRF's from force to modal coordinates. Away from natural frequencies, the sensor outputs may contain a little contribution from unwanted modes. To eliminate this sensitivity to unwanted modes, the adaptive design procedure described in this chapter still needs refinement.